Letter

Hydrodynamic interactions between rough surfaces

Ehud Yariv [1,2] Rodolfo Brandão [1] David K. Wood [3] Hannah Szafraniec [3]
John M. Higgins [4] Parisa Bazazi [5] Philip Pearce [6] and Howard A. Stone [1,*]

[1]*Department of Mechanical and Aerospace Engineering, Princeton University, Princeton, New Jersey 08544, USA*

[2]*Department of Mathematics, Technion — Israel Institute of Technology, Haifa 32000, Israel*

[3]*Department of Biomedical Engineering, University of Minnesota, Minneapolis, Minnesota 55455, USA*

[4]*Center for Systems Biology and Department of Pathology, Massachusetts General Hospital, and Department of Systems Biology, Harvard Medical School, Boston, Massachusetts 02114, USA*

[5]*Colorado School of Mines, Golden, Colorado 80401, USA*

[6]*Department of Mathematics, University College London, London WC1H 0AY, United Kingdom*

(Received 27 September 2023; accepted 8 February 2024; published 11 March 2024; corrected 20 March 2024)

In the study of particle suspensions, away from the jamming threshold, it is common to interpret the effective viscosity in terms of the volume fraction, neglecting roughness effects. Here we show that particle roughness can significantly modify viscous dissipation in configurations that represent fixed volume-fraction conditions. We derive a hydrodynamic model for the forced interaction of a two-dimensional particle, where roughness is represented by a periodic corrugation, with an adjacent wall. In particular, we address the limit of small nominal particle-wall separation, with the corrugation amplitude comparable with said separation. A lubrication analysis provides the rectilinear and angular velocities of the particle as functions of the instantaneous angular configuration. The particle may either translate while rotating or become "locked" in a specific phase and translate without rotation. The time-averaged rectilinear velocity, which is the object of interest, is a purely geometric quantity, obtained without the need to address any time dynamics.

DOI: 10.1103/PhysRevFluids.9.L032301

Introduction. A wide range of industrial, geophysical, and biological flows involve particulate suspensions, from inks and pastes to magma, mucus, and blood [1,2]. Thus, understanding particulate suspension rheology is important for both industrial applications and human health. Traditionally, rheological models of suspensions have assumed that constituent particles are smooth spheres. In such models, hydrodynamic interactions between particles dominate emergent suspension rheology, because lubrication forces resist direct contacts. A more recent literature has explored the effect of surface roughness of particles and boundaries, which have been assumed to promote frictional solid-solid contacts [1–7]. In particular, the theoretical model of da Cunha and Hinch [8] accounts for roughness by modifying the mobility functions when a prescribed critical separation is reached, the modification being based upon existing mobility calculations for a locked pair of particles. That model successfully explained the experimental findings of Blanc *et al.* [9,10].

Following da Cunha and Hinch [8], it became desirable to understand the lubrication interactions between the asperities. In present models, lubrication interactions are typically considered to be independent of surface roughness [3–6,11] or are included using *ad hoc* approaches [7]. Studies

*Corresponding author: hastone@princeton.edu

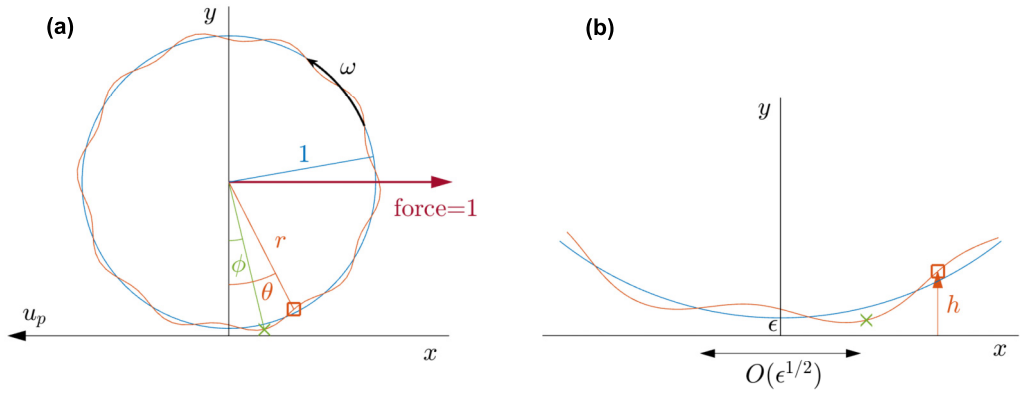

FIG. 1. (a) Dimensionless geometry showing both the nominal and corrugated shapes. (b) The gap region. The cross symbol, at angle ϕ relative to the vertical, indicates the conceptual marker. The square symbol, at angle θ relative to the vertical, indicates a generic boundary point. The parameters are $\epsilon = 0.05$, $A = 0.7$, $n = 10$, and $n\phi = 3\pi/4$, with $S(\cdot) = \cos(\cdot)$.

investigating the role of roughness through hydrodynamic interactions have been confined to numerical calculations at volume fractions near jamming, which either explicitly simulate corrugated particles [12,13] or assume smooth particles subject to modified hydrodynamic forces [13]. In general, it is not well understood how lubrication interactions between rough particles contribute to overall dissipation in particulate suspensions across a wide range of volume fractions.

The role of roughness therefore remains poorly characterized. Recently, particle roughness has been found to reduce shear-induced diffusivity in non-Brownian suspensions at volume fractions higher than around 0.25 [7], in contrast with lower volume fractions where roughness increases dispersion [8]. A striking example of particulate properties affecting macroscopic rheology is sickle cell disease, in which diseased red blood cells are affected by the polymerization of hemoglobin, causing them to become rigid and misshapen when deoxygenated [14–16]. Recent rheological measurements appear to indicate that suspensions of sickled cells form a pluglike flow even when the volume fraction is estimated to be around 0.3 [17], far below the jamming fraction [18]. Motivated by these recent studies, we hypothesize that perturbed lubrication interactions caused by surface roughness, of amplitude small compared to the typical particle radius, could potentially be significant even at modest volume fractions, since the roughness amplitude can then be comparable to the typical film thickness separating the particles.

In this Letter, we study a model problem highlighting the significant hydrodynamic effects expected when small surface roughness is included in thin-film models representative of suspension flows. In particular, we highlight the potential impact of roughness on a model flow with relative motion of two surfaces, in which the corrugation amplitude is comparable to the separation distance. To this end, we examine the forced motion of a nominally circular particle at a fixed nominal separation from a solid wall.

Model problem. Consider a rough 2D particle that is placed within a viscous fluid (viscosity μ^*) near a planar rigid wall [Fig. 1(a)]. Our interest is in the motion of the particle due to an external force (per unit length) F^* parallel to the wall. In this idealized configuration, the particle centroid is prevented (by external means) from translating perpendicular to the wall. It is nonetheless free to translate parallel to the wall and rotate. We seek the difference between the average rectilinear velocity and that of a comparable smooth particle.

In modeling the particle roughness, we envision a corrugation about a nominal circular shape of radius a^*. Consistent with the model problem, the distance between the nominal shape and the wall is fixed, say, ϵa^*. The corrugation is generically described using a 2π-periodic function $\mathcal{S}$ with zero mean, an amplitude $\epsilon a^* A$, and a "wave number" $n \in \mathbb{N}$; the nominal shape is retrieved by setting

$A = 0$. Since the corrugation is intrinsic to the particle, its description in a nonrotating reference frame is facilitated by referring to a conceptual "marker" on the particle boundary. Thus, measuring angles counterclockwise in the manner specified in Fig. 1(a), we consider a generic boundary point at angle θ; its distance from the particle centroid (which coincides with the center of the nominal circular shape) is $a^* r$, where

$$r = 1 + \epsilon A \mathcal{S}[n(\theta - \phi)], \tag{1}$$

in which ϕ is the instantaneous angle of the marker (indicated by the cross symbol in Fig. 1). Imposing $A < 1$, we may specify without loss of generality that $\max|\mathcal{S}| = 1$. The period of the function $\mathcal{S}[n(\theta - \phi)]$ is $2\pi/n$. Due to that periodicity, it suffices to consider the range

$$-\pi/n < \phi < \pi/n. \tag{2}$$

The "phase" ϕ uniquely characterizes the instantaneous configuration of the rough particle.

Instantaneous motion. We consider a small particle, such that the flow is governed by the Stokes equations (low Reynolds numbers) [19]. The solution to the Stokes equations is determined by the instantaneous geometry: in particular, the condition of a torque-free particle under a prescribed external force uniquely sets the angular velocity ω^* of the particle and the rectilinear velocity u_p^* of its centroid. We employ a dimensionless notation, where length variables are normalized by a^*; forces and torques (per unit length) by F^* and a^*F^*, respectively; velocities and angular velocities by F^*/μ^* and $F^*/\mu^* a^*$, respectively; and stresses (and pressure) by F^*/a^*. We conveniently employ (x, y, z) Cartesian coordinates (see Fig. 1) in a nonrotating reference attached to the particle centroid. In this system, the wall moves with velocity $-u_p\hat{\mathbf{e}}_x$ ($u_p = \mu^* u_p^*/F^*$) while the particle rotates with angular velocity $\hat{\mathbf{e}}_z\omega$ ($\omega = \mu^* a^* \omega^*/F^*$). The external force on the particle is $\hat{\mathbf{e}}_x$, and there is no external torque.

The linearity of the governing Stokes equations motivates the specification of two auxiliary drag problems. In the "rotation problem" the particle rotates with velocity $\hat{\mathbf{e}}_z$ and the wall is stationary. This motion results in the drag force $-f_{\mathrm{rot}}\hat{\mathbf{e}}_x$ and the hydrodynamic torque $-g_{\mathrm{rot}}\hat{\mathbf{e}}_z$. (Both problems also give rise to a normal force in the y direction, which is of no interest as the particle is constrained to translate parallel to the wall.) In the "translation problem" the particle is stationary and the wall moves with velocity $-\hat{\mathbf{e}}_x$; this results in the drag force $-f_{\mathrm{tr}}\hat{\mathbf{e}}_x$ and the hydrodynamic torque $-g_{\mathrm{tr}}\hat{\mathbf{e}}_z$. The four pertinent hydrodynamic coefficients, $\{f_{\mathrm{rot}}, g_{\mathrm{rot}}, f_{\mathrm{tr}}, g_{\mathrm{tr}}\}$, are functions of the geometric parameters, ϵ, A, and n (and the shape $\mathcal{S}$) as well as the phase ϕ. Due to Stokes-flow symmetry [19],

$$f_{\mathrm{rot}} = g_{\mathrm{tr}}. \tag{3}$$

For smooth (circular) particles, it so happens that these coupling terms vanish [20], but that particular simplification is not expected in the general case $A > 0$.

Once the hydrodynamic coefficients are obtained, we can consider the mobility problem for a torque-free particle that experiences an external unit force. Using linearity, the velocities u_p and ω of the particle in the original problem are thus determined from the equilibrium conditions

$$f_{\mathrm{tr}} u_p + f_{\mathrm{rot}}\omega = 1, \quad g_{\mathrm{tr}} u_p + g_{\mathrm{rot}}\omega = 0. \tag{4}$$

Average velocity. Denoting the position of the particle centroid (in a laboratory reference frame) as x_p, we have the kinematic equations

$$\frac{dx_p}{dt} = u_p, \tag{5a}$$

$$\frac{d\phi}{dt} = \omega, \tag{5b}$$

where time t is normalized by $\mu^* a^*/F^*$. We note that both u_p and ω are functions of the phase ϕ, but not of x_p. Thus, (5b) can be integrated. With $dt = d\phi/\omega$, the time to rotate an angle $2\pi/n$ is

$T = \int_{-\pi/n}^{\pi/n} d\phi/\omega$. During that time, the particle traverses a distance $\int_0^T u_p\, dt$, or, reverting to $d\phi$, $\int_{-\pi/n}^{\pi/n} u_p\, d\phi/\omega$. The average velocity, $\bar{u}_p$, is given by the ratio of that distance to T, namely,

$$\bar{u}_p = \frac{\int_{-\pi/n}^{\pi/n} u_p\, d\phi/\omega}{\int_{-\pi/n}^{\pi/n} d\phi/\omega}. \tag{6}$$

Note that $\bar{u}_p$ is a purely *geometric* quantity: the two integrands in (6) may be considered as known functions of the geometry and phase ϕ.

Lubrication limit. The preceding discussion imposes no restriction on the nominal gap width ϵ. We now consider the near-contact limit $\epsilon \ll 1$. That limit represents scenarios where the volume fraction is fixed to leading order, reflecting our goal of assessing the relative impact of surface roughness. Moreover, the hydrodynamic forces are dominated by the flow in the narrow gap, where a lubrication mechanism gives rise to large shear stresses and even larger pressure variations. Thus, to leading order we need to resolve the flow in the gap region, where $\theta \approx x \ll 1$.

With the distance h from the boundary to the wall being $h = 1 + \epsilon - r\cos\theta$ [see Fig. 1(b)], we find using (1) that $h \approx \epsilon(1 - A\mathcal{S}) + x^2/2$ in the gap. The pertinent length scale in the x direction is clearly $\epsilon^{1/2}$, which is familiar from lubrication theory. The distinguished limit is where the corrugation wavelength is comparable with the extent of the gap, implying that n is of order $\epsilon^{-1/2}$. We therefore employ the rescaled wave number $N = \epsilon^{1/2} n$. Since $\phi = O(1/n)$ [recall (2)], we hereafter also employ the rescaled phase $\Phi = n\phi$, which satisfies $-\pi < \Phi < \pi$. Defining the stretched Cartesian coordinates $X = \epsilon^{-1/2} x$ and $Y = \epsilon^{-1} y$, the particle boundary is $Y = H(X) + \cdots$, wherein

$$H(X) = 1 + \frac{X^2}{2} - A\mathcal{S}(NX - \Phi). \tag{7}$$

The parameters used in Fig. 1 have been chosen to represent the above scaling. Thus, with $\epsilon = 0.05$ and $n = 10$, N is approximately 2.

Lubrication analysis. Consider the two auxiliary drag problems. In the lubrication approximation for $\epsilon \ll 1$, given the chosen rescaling, the x component u of the fluid velocity is of order unity in the gap, while the pressure $p = O(\epsilon^{-3/2})$ there [20]. We accordingly write $u = U$ and $p = \epsilon^{-3/2} P$. The resulting forces and torque coefficients are of order $\epsilon^{-1/2}$. At that leading order, both the torque and the force are affected by the $O(\epsilon^{-1})$ shear stress; the force is also affected by the $O(\epsilon^{-3/2})$ pressure. We therefore write

$$f_{\rm tr} = \epsilon^{-1/2} F_{\rm tr}, \quad g_{\rm tr} = \epsilon^{-1/2} G_{\rm tr}, \quad f_{\rm rot} = \epsilon^{-1/2} F_{\rm rot}, \quad g_{\rm rot} = \epsilon^{-1/2} G_{\rm rot}, \tag{8}$$

where the rescaled coefficients are provided as quadratures over the particle boundary [20]

$$G_{\rm tr,rot} = \int_{-\infty}^{\infty} \left(\frac{\partial U}{\partial Y} \right)_{Y=H} dX, \tag{9a}$$

$$F_{\rm tr,rot} = \int_{-\infty}^{\infty} \left(\frac{\partial U}{\partial Y} + H' P \right)_{Y=H} dX, \tag{9b}$$

in which the "edges" of the gap region are at $X = \pm\infty$ and the prime denotes differntiation. In these quadratures, U and P are the appropriate fields for either the rotational or translational problem.

The fields U and P satisfy the Stokes equations, which at leading order reduce to

$$\frac{\partial P}{\partial X} = \frac{\partial^2 U}{\partial Y^2}, \quad \frac{\partial P}{\partial Y} = 0. \tag{10}$$

The latter implies that P is a function of X alone, say, $P(X)$; integration of the former yields $U = \frac{1}{2} P'(X) Y^2 + C(X) Y + D(X)$, where the unknown functions C and D are to be determined from

the appropriate boundary conditions on U, and $P'(X)$ is yet undetermined. Rather than using the continuity equation, we employ an integral balance [21], requiring that the volumetric flux through the gap, $Q = \int_0^H U\, dY$, is independent of X, and is therefore a constant. (This is the reason for the use of a comoving frame in the translation problem.) This procedure determines the *function* $P'(X)$ in terms of the *scalar* unknown Q.

The unknown flux Q, in turn, is determined by the requirement $\int_{-\infty}^{\infty} P'\, dX = 0$, representing the need of the gap pressure to match the $O(1)$ pressure outside. This requirement reads

$$P(\pm\infty) = 0. \tag{11}$$

With Q determined using (11), $P'(X)$ as well as $C(X)$ and $D(X)$ may be considered as known (in closed form) for arbitrary $\mathcal{S}$. In contrast to classical lubrication flows [20], here we cannot integrate $P'(X)$ to obtain $P(X)$ explicitly (cf. [22]). This is not required, however, since integration by parts in conjunction with (11) allows replacing the integrand of (9b) by $(\partial U/\partial Y)_{Y=H} - HP'$.

Making use of the above procedure we now address the rotation problem, where $U = 0$ at $Y = 0$ and $U = 1$ at $Y = H$. This readily yields

$$G_{\mathrm{rot}} = 4I_1 - \frac{3I_2^2}{I_3}, \quad F_{\mathrm{rot}} = \frac{3I_2^2}{I_3} - 2I_1, \tag{12}$$

wherein the quadratures

$$I_m = \int_{-\infty}^{\infty} \frac{dX}{H^m} \tag{13}$$

depend upon A, N, Φ, and the shape function $\mathcal{S}$ [recall (7)]. The solution of the translation problem, where $U = 0$ at $Y = 0$ and $U = -1$ at $Y = H$, gives

$$G_{\mathrm{tr}} = F_{\mathrm{rot}}, \tag{14}$$

as required by (3). Coincidentally, it also gives

$$F_{\mathrm{tr}} = G_{\mathrm{rot}}. \tag{15}$$

For future reference, we note that in the smooth particle case ($A = 0$) the pure numbers I_m are readily obtained as $I_1 = \pi\sqrt{2}$, $I_2 = \pi/\sqrt{2}$, and $I_3 = 3\pi/4\sqrt{2}$; from (12)–(15) we then reproduce the classical result for a smooth circular particle moving parallel to a wall [20]: $G_{\mathrm{rot}} = F_{\mathrm{tr}} = 4\pi/\sqrt{2}$ and $F_{\mathrm{rot}} = G_{\mathrm{tr}} = 0$; in particular, such a particle experiences no torque and hence does not rotate. In the present context of a rough particle, where the shape function (7) applies, no such general simplification is available.

Results. With the $O(\epsilon^{-1/2})$ hydrodynamic coefficients (8), the balances (4) necessitate $O(\epsilon^{1/2})$ velocities. Writing $u_p = \epsilon^{1/2}U_p$ and $\omega = \epsilon^{1/2}\Omega$, these balances are replaced by

$$F_{\mathrm{tr}}U_p + F_{\mathrm{rot}}\Omega = 1, \quad G_{\mathrm{tr}}U_p + G_{\mathrm{rot}}\Omega = 0. \tag{16}$$

In particular, for the smooth case $A = 0$ we obtain $\Omega = 0$ and

$$U_p(A = 0) = \frac{\sqrt{2}}{4\pi}. \tag{17}$$

We emphasize that we have factored out the roughness scale ϵ. We therefore have a scheme for the determination of rigid-body velocities as functions of the two geometric parameters A and N, the function $\mathcal{S}(\cdot)$, and the phase Φ. It entails numerically evaluating the integrals I_m ($m = 1, 2, 3$) using (7). Subsequently, (12) is employed to obtain the hydrodynamic coefficients. Then, recalling the symmetries (14)–(15), the linear system (16) is inverted.

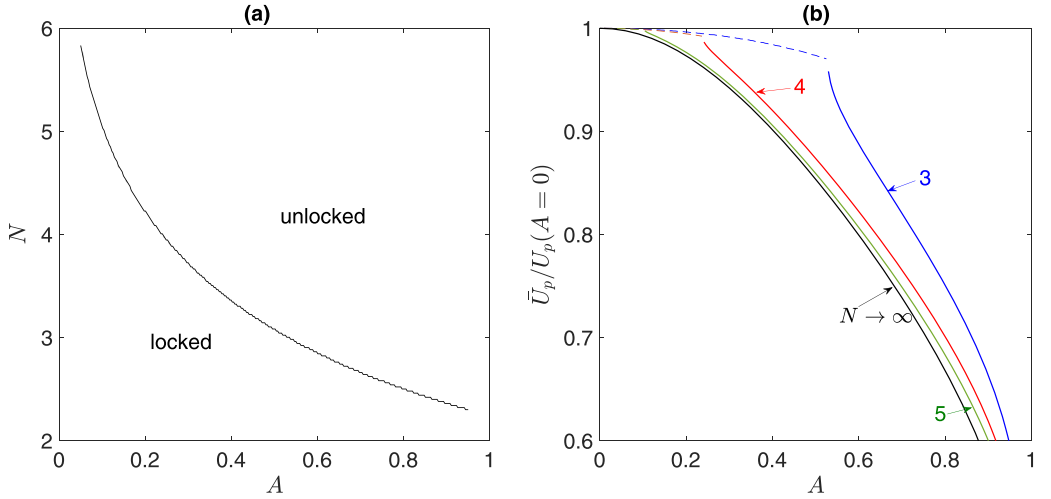

FIG. 2. Results for $S(\cdot) = \cos(\cdot)$. (a) Phase diagram showing the regions in the A–N plane where the particle is in the locked and unlocked states. (b) Variation of $\bar{U}_p/U_p(A = 0)$ as a function of A for the indicated values of N. The dashed portions of the curves indicate a locked state. The limit $N \to \infty$, obtained using the homogenized integrals (20), is also shown.

In principle, the above scheme can be performed for any phase $\Phi \in (-\pi, \pi)$. The associated mean velocity follows from (6),

$$\bar{U}_p = \frac{\int_{-\pi}^{\pi} U_p \, d\Phi/\Omega}{\int_{-\pi}^{\pi} d\Phi/\Omega}. \tag{18}$$

The quantity of interest is the mean velocity $\bar{U}_p$, normalized by the velocity (17) of a smooth particle.

We recall that for $A = 0$ the absence of coupling implies that $\Omega = 0$. Such a situation can also occur for $A > 0$. As an illustration, consider $A \ll 1$. A straightforward calculation for $S(\cdot) = \cos(\cdot)$ gives [cf. (17)]

$$U_p = \frac{\sqrt{2}}{4\pi} + O(A), \tag{19a}$$

$$\Omega = A \frac{e^{-N\sqrt{2}} N^3}{6\pi} \cos\Phi + O(A^2), \tag{19b}$$

so, to leading order in A, Ω vanishes at $\Phi = \pm\pi/2$, corresponding to a geometry where the gap width at $x = 0$ coincides with ϵ [recall (7)]. A scenario (namely, a given pair of A and N) where there exists a phase Φ at which $\Omega = 0$ implies that the particle would get "locked" in that phase. While we have no predictive theoretical argument for the formation of locked states at finite A values, our computational scheme allows one to observe these states. In Fig. 2(a) we show a phase diagram in the A–N plane, delineating the region where the particle gets locked and the region where it does not get locked. As A becomes small, the range of locked N values increases indefinitely, in agreement with (19b).

For a locked pair (A, N), expression (18) becomes indeterminate as both the numerator and denominator increase without bound. Recalling the geometric interpretation of (18) as a mean velocity, however, it is evident that the limit $\bar{U}_p$ simply coincides with the instantaneous value of U_p at the locked state. With that interpretation, we may evaluate $\bar{U}_p$ for any (A, N) pair. In Fig. 2(b) we illustrate the variation with A of the mean velocity, normalized by $U_p(A = 0)$, as given by (17).

We observe that the numerical data collapse onto a limiting curve as N increases. This can be rationalized by noting that, as $N \to \infty$, the geometric details of the roughness are "averaged out," thus leading to a homogenized description of the hydrodynamics. To gain further insight into this limit, we now employ the method of multiple scales [23]. Accordingly, we define a shifted "fast variable" $\chi = NX - \Phi$ and rewrite the gap thickness (7) as $H(X, \chi) = 1 + X^2/2 - AS(\chi)$, where X and χ are treated as independent. In the limit $N \to \infty$, the integrals (13) attain the asymptotic form [24]

$$I_m \approx \int_{-\infty}^{\infty} \left\langle \frac{1}{H^m} \right\rangle_\chi dX \quad \text{where} \quad \left\langle \frac{1}{H^m} \right\rangle_\chi = \frac{1}{2\pi} \int_0^{2\pi} \frac{d\chi}{H^m}. \tag{20}$$

Note that, due to the periodicity of the shape, the homogenized integrals are independent of Φ. Using (20), we can calculate the homogenized hydrodynamic coefficients (12), and then using (16), the homogenized velocities. Since the homogenized velocities are also independent of Φ, the time average (18) is redundant and $\bar{U}_p \approx U_p$. The homogenized speed as a function of A is indicated by the black curve ($N \to \infty$) in Fig. 2(b).

Since the lubrication approximation breaks down when the wavelength is comparable with the gap, the homogenization scheme is valid for $1 \ll N \ll \epsilon^{-1/2}$. Importantly, our homogenized description is not equivalent to that of a smooth particle with a larger "effective" radius. This can be verified explicitly for $S(\cdot) = \cos(\cdot)$, where the homogenized integrands $\langle 1/H^m \rangle_\chi$ can be calculated in closed form. Furthermore, a smooth two-dimensional particle does not rotate, whereas our analysis reveals that sufficiently rough particles do rotate. This again illustrates the critical role of surface roughness in the hydrodynamics of suspended particles.

Concluding remarks. In the idealized 2D model considered herein, the hydrodynamic loads in the small-gap limit are dominated by a "local" contribution from the gap, as the "global" contribution from the particle-scale flow is subdominant. The resulting hydrodynamic loads are proportional to $\epsilon^{-1/2}$, where ϵ is the ratio between the particle-wall separation and particle radius. On that scale, corrugation results in a significant relative effect.

In principle, the analysis in the present Letter can be reapplied to the (more realistic) 3D geometry of a rough spherical particle. In addition to the obvious technical complications, the small-gap limit is slightly intricate [25,26]. Thus, the lubrication analysis in 3D gives rise to a local contribution that diverges logarithmically with the distance to the "edge" of the gap region. That superfluous divergence is canceled out by the global contribution. This cancellation represents an "intermediate" scaling, where the contribution to the hydrodynamic loads is neither local nor global, but is rather dominated by the transition between the two asymptotic regions [23]. Thus, the hydrodynamic loads comprise both an $O(1)$ and an $O(\ln \epsilon)$ term.

As the global contribution is unaffected at leading order by the corrugation, it is readily provided by the classical analyses of O'Neill and coworkers [25,26]. It follows that the $O(\ln \epsilon)$ load coincides with that on a smooth particle, as originally calculated by Goldman, Cox, and Brenner [27]. The roughness would affect only the $O(1)$ load. Considering $O(\ln \epsilon)$ terms on par with $O(1)$ terms [28], we then anticipate that, just as in the 2D case analyzed above, a small corrugation would result in an $O(1)$ *relative* modification to the mean velocity. Given the technical complications associated with the need to address two different asymptotic regions, we find the 2D problem more illustrative.

The theoretical results in this paper suggest a new role for particle roughness in determining the emergent properties of particulate suspensions. We have identified how, within the framework of lubrication interactions between a circular particle and a plane wall, roughness causes relative $O(1)$ changes to the translation and rotation speed of the particle. To mimic particle confinement in suspension flows, we have considered a particle with a fixed separation distance from the wall, chosen to represent typical particle-particle distances in suspensions of modest volume fraction; in practice, this distance will be set by numerous fluid [3,7,8] and solid interactions [5] between multiple particles. Our findings suggest that perturbed hydrodynamic interactions caused by roughness

could provide a significant contribution to the viscous response of particulate suspensions for a wide range of volume fractions, even those well removed from the jamming transition.

Acknowledgments. D.K.W., J.M.H., and H.A.S. are supported by the NHLBI under Grant No. R01HL132906. P.P. is supported by a UKRI Future Leaders Fellowship (MR/V022385/1). R.B. is supported by a Princeton Presidential Postdoctoral Research Fellowship.

[1] C. Ness, R. Seto, and R. Mari, The physics of dense suspensions, Annu. Rev. Condens. Matter Phys. **13**, 97 (2022).

[2] É. Guazzelli and O. Pouliquen, Rheology of dense granular suspensions, J. Fluid Mech. **852**, P1 (2018).

[3] J. R. Smart, S. Beimfohr, and D. T. Leighton, Measurement of the translational and rotational velocities of a noncolloidal sphere rolling down a smooth inclined plane at low Reynolds number, Phys. Fluids **5**, 13 (1993).

[4] H. J. Wilson and R. H. Davis, The viscosity of a dilute suspension of rough spheres, J. Fluid Mech. **421**, 339 (2000).

[5] K. P. Galvin, Y. Zhao, and R. H. Davis, Time-averaged hydrodynamic roughness of a noncolloidal sphere in low Reynolds number motion down an inclined plane, Phys. Fluids **13**, 3108 (2001).

[6] A. K. Townsend and H. J. Wilson, Frictional shear thickening in suspensions: The effect of rigid asperities, Phys. Fluids **29**, 121607 (2017).

[7] H. Zhang, P. Pham, B. Metzger, D. I. Kopelevich, and J. E. Butler, Effect of particle roughness on shear-induced diffusion, Phys. Rev. Fluids **8**, 064303 (2023).

[8] F. R. Da Cunha and E. J. Hinch, Shear-induced dispersion in a dilute suspension of rough spheres, J. Fluid Mech. **309**, 211 (1996).

[9] F. Blanc, F. Peters, and E. Lemaire, Experimental signature of the pair trajectories of rough spheres in the shear-induced microstructure in noncolloidal suspensions, Phys. Rev. Lett. **107**, 208302 (2011).

[10] F. Blanc, E. Lemaire, A. Meunier, and F. Peters, Microstructure in sheared non-Brownian concentrated suspensions, J. Rheol. **57**, 273 (2013).

[11] R. V. More and A. M. Ardekani, A constitutive model for sheared dense suspensions of rough particles, J. Rheol. **64**, 1107 (2020).

[12] S. Jamali and J. F. Brady, Alternative frictional model for discontinuous shear thickening of dense suspensions: Hydrodynamics, Phys. Rev. Lett. **123**, 138002 (2019).

[13] M. Wang, S. Jamali, and J. F. Brady, A hydrodynamic model for discontinuous shear-thickening in dense suspensions, J. Rheol. **64**, 379 (2020).

[14] T. Itoh, S. Chien, and S. Usami, Deformability measurements on individual sickle cells using a new system with pO2 and temperature control, Blood **79**, 2141 (1992).

[15] H. Hiruma, C. T. Noguchi, N. Uyesaka, S. Hasegawa, E. J. Blanchette-Mackie, A. N. Schechter, and G. P. Rodgers, Sickle cell rheology is determined by polymer fraction—Not cell morphology, Am. J. Hematol. **48**, 19 (1995).

[16] D. P. Papageorgiou, S. Z. Abidi, H.-Y. Chang, X. Li, G. J. Kato, G. E. Karniadakis, S. Suresh, and M. Dao, Simultaneous polymerization and adhesion under hypoxia in sickle cell disease, Proc. Natl. Acad. Sci. USA **115**, 9473 (2018).

[17] H. M. Szafraniec, J. M. Valdez, E. Iffrig, W. A. Lam, J. M. Higgins, P. Pearce, and D. K. Wood, Feature tracking microfluidic analysis reveals differential roles of viscosity and friction in sickle cell blood, Lab Chip **22**, 1565 (2022).

[18] A. Baule, F. Morone, H. J. Herrmann, and H. A. Makse, Edwards statistical mechanics for jammed granular matter, Rev. Mod. Phys. **90**, 015006 (2018).

[19] J. Happel and H. Brenner, *Low Reynolds Number Hydrodynamics* (Springer Netherlands, Dordrecht, 1983), Vol. 1.

[20] D. J. Jeffrey and Y. Onishi, The slow motion of a cylinder next to a plane wall, Q. J. Mech. Appl. Math. **34**, 129 (1981).
[21] S. H. Davis, The importance of being thin, J. Eng. Math. **105**, 3 (2017).
[22] U. Kaynan and E. Yariv, Stokes resistance of a cylinder near a slippery wall, Phys. Rev. Fluids **2**, 104103 (2017).
[23] E. J. Hinch, *Perturbation Methods* (Cambridge University Press, Cambridge, 1991).
[24] G. Allaire, Homogenization and two-scale convergence, SIAM J. Math. Anal. **23**, 1482 (1992).
[25] M. E. O'Neill and K. Stewartson, On the slow motion of a sphere parallel to a nearby plane wall, J. Fluid Mech. **27**, 705 (1967).
[26] M. D. A. Cooley and M. E. O'Neill, On the slow rotation of a sphere about a diameter parallel to a nearby plane wall, J. Inst. Math. Applics. **4**, 163 (1968).
[27] A. J. Goldman, R. G. Cox, and H. Brenner, Slow viscous motion of a sphere parallel to a plane wall—I. Motion through a quiescent fluid, Chem. Eng. Sci. **22**, 637 (1967).
[28] M. Van Dyke, *Perturbation Methods in Fluid Mechanics* (Academic Press, New York, 1964).

Correction: The relation sign in Equation (9b) was inadvertently deleted during the production stage and has been fixed. The subscripts "tr" and "rot" were inconsistently presented by the production operator and have been fixed.